Sensors and Actuators A 241 (2016) 245–253

Contents lists available at ScienceDirect

Sensors and Actuators A: Physical

journal homepage: www.elsevier.com/locate/sna

# Electrothermal actuation of vanadium dioxide for tunable capacitors and microwave filters with integrated microheaters[☆]

Wolfgang A. Vitale[a,*], Luca Petit[a], Clara F. Moldovan[a], Montserrat Fernández-Bolaños[a], Antonio Paone[b], Andreas Schüler[b], Adrian M. Ionescu[a]

[a] NanoLAB, École Polytechnique Fédérale de Lausanne (EPFL), CH-1015 Lausanne, Switzerland
[b] Solar Energy and Building Physics Laboratory (LESO-PB), EPFL, CH-1015 Lausanne, Switzerland

ARTICLE INFO

*Article history:*
Received 29 September 2015
Received in revised form 9 December 2015
Accepted 14 January 2016
Available online 19 January 2016

*Keywords:*
Vanadium dioxide
Electrothermal actuation
Microheaters
Metal-insulator transition
Radio frequency
Tunable capacitors
Microwave filters

ABSTRACT

We report the fabrication, modeling and characterization of novel microwave tunable capacitors based on the metal-insulator transition (MIT) of Vanadium Dioxide ($VO_2$) as a future replacement solution for microelectromechanical capacitive switches. We present the advantages of $VO_2$-based capacitors over alternative technologies for microwave reconfigurable electronics in terms of ease of integration, design and performance at high frequency. We show the potential of the proposed devices for RF reconfigurable electronics by fabricating a tunable bandstop filter (22.5–19.8 GHz) with insertion loss <2 dB up to 40 GHz. We propose an alternative method for actuation of the $VO_2$ active regions by employing integrated microheaters and we study their effect on the filter performance by electrothermal and electromagnetic simulations.

## 1. Introduction

Microwave tunable filters are among the most important components in wireless communications systems, due to their ability to control the spectral profile of the transmitter and the receiver while excluding undesirable narrowband signals, eliminating the need to employ bulky filter banks. The development of a low-cost, miniaturized, reliable technology for analog and digital control of microwave filters is of foremost importance for the next generations of wireless communication systems.

Several technologies have been proposed for the realization of frequency-agile filters. Some of the most commonly employed solutions are semiconductor radio frequency (RF) switches and varactors, which are limited by insertion loss at high frequency [1], and RF micro-mechanical systems (MEMS), affected by reliability issues and complexity of integration [2].

Vanadium dioxide ($VO_2$) is a functional oxide that has attracted increasing research interest in the last few years as a new technological solution for reconfigurable electronics. The physical mechanism exploited in $VO_2$ for reconfigurable devices is the metal-insulator transition (MIT); $VO_2$ undergoes a structural transition from monoclinic to tetragonal phase above the transition temperature $T_{MIT}$ (~68 °C), leading to an abrupt decrease in resistivity, which can reach up to 5 orders of magnitude in bulk $VO_2$ [3] and epitaxial thin films on sapphire [4].

The resistivity modulation in $VO_2$ has been exploited to fabricate compact RF switches with high reliability and low insertion loss independent of frequency [5]. However, the application of $VO_2$-based RF switches for microwave tunable filters has been limited to frequencies ~10 GHz [6–8] because of the relatively high parasitic capacitance between the metal contacts [9]. We introduce novel $VO_2$-based tunable capacitors as an alternative solution, presenting their advantages in terms of ease of integration, design and performance at high frequency. The proposed devices overcome the frequency limitations of $VO_2$-based RF switches while keeping their advantages in terms of low insertion loss. We exploit the $VO_2$ tunable capacitors for the design and fabrication of CMOS-compatible thermally actuated microwave tunable bandstop filters working in the K band, and we study by electrothermal and electromagnetic simulations an alternative method for actuation by integrating microheaters for local heating of the $VO_2$ active regions. Table 1 compares the performance of the proposed devices to the

---

[☆] Selected paper from Transducers 2015 conference, June 21–25, 2015, Alaska, USA.

[*] Corresponding author.
*E-mail addresses:* wolfgang.vitale@epfl.ch, wolfgang.vitale@gmail.com (W.A. Vitale).

http://dx.doi.org/10.1016/j.sna.2016.01.027

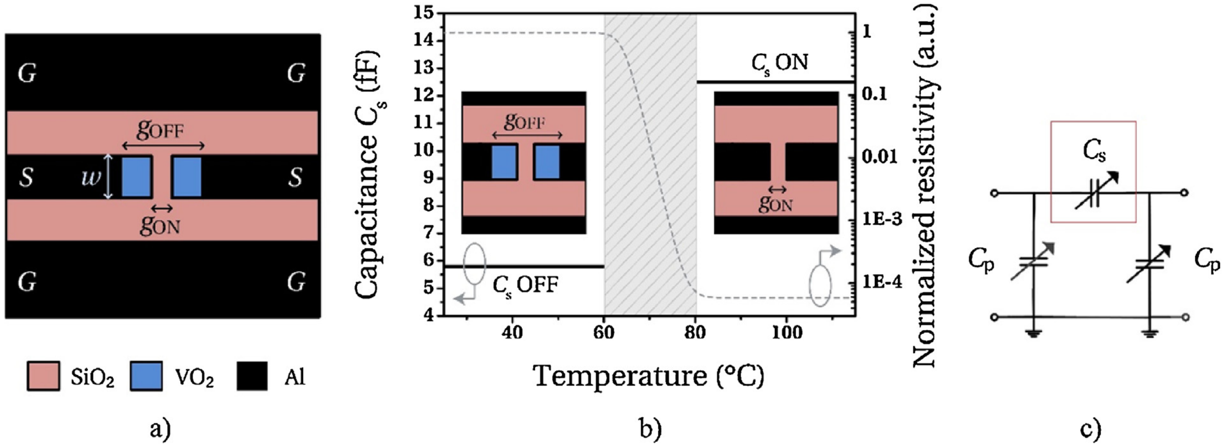

**Fig. 1.** (a) Schematic diagram of a VO$_2$ tunable capacitor loaded on a coplanar waveguide in series configuration. The capacitive gap between the signal lines can be tuned from $g_{OFF}$ (VO$_2$ in insulating state) to $g_{ON}$ (VO$_2$ in conducting state). (b) Effects of thermal actuation on the resistivity and series capacitance. The resistivity transition occurs mostly in the shaded area, outside of which a low and a high capacitance states are well defined. (c) Equivalent lumped circuit.

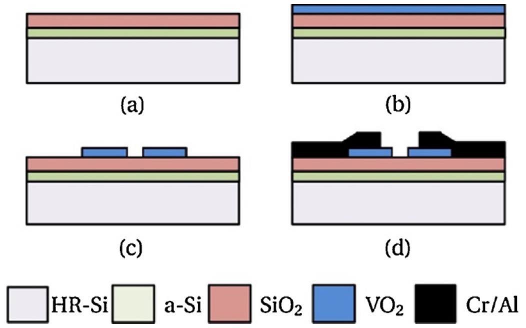

**Fig. 2.** Main steps of the fabrication process for VO$_2$ tunable capacitors. (a) LPCVD of 300 nm amorphous silicon and 500 nm SiO$_2$ on HR-Si substrate. (b) Sputtering deposition of 360 nm VO$_2$. (c) Patterning of VO$_2$ by optical lithography and ion beam etching. (d) 20/300 nm Cr/Al evaporation patterned by lift-off.

one of previously reported VO$_2$ tunable filters, with clear improvements in terms of frequency range of operation and tunability.

## 2. VO$_2$ tunable capacitors

### 2.1. Design

The working principle of the VO$_2$ tunable capacitor consists in exploiting the MIT in VO$_2$ to tune the length of capacitive gaps in transmission lines. For instance, a possible configuration is depicted in the diagram in Fig. 1(a), where a pair of VO$_2$ patterned regions is used to adjust the length of a series capacitive gap in a coplanar waveguide (CPW). The length of the capacitive gap depends on the VO$_2$ phase, varying from $g_{OFF}$ at room temperature to $g_{ON}$ at $T > T_{MIT}$, when VO$_2$ transitions to the metallic state. The effects of the MIT on the VO$_2$ capacitor are qualitatively illustrated in Fig. 1(b). Increasing the temperature above $T_{MIT}$ induces a decrease in VO$_2$ resistivity with magnitude and steepness depending on the quality of the VO$_2$ film. The series capacitor $C_s$ switches from a low value when the film is insulating to a high value when the film is highly conducting.

Symmetric series gaps in CPWs are accurately modeled by a Π circuit, including parasitic capacitors $C_p$ for the parallel branches. Therefore the VO$_2$ tunable capacitor can be modeled by the equivalent lumped circuit shown in Fig. 1(c), where the tunability is due to the MIT in VO$_2$: the decrease in length from $g_{OFF}$ to $g_{ON}$ leads to an increase in $C_s$ and a decrease in $C_p$ [10].

### 2.2. Fabrication

Fig. 2 illustrates the main steps of the fabrication process employed for the devices characterized in this work. We use as substrates 4″ high-resistivity silicon (HR-Si) wafers (> 10 kΩ cm) in order to ensure low dielectric loss while keeping CMOS compatibility. The process starts with the low-pressure chemical-vapor-deposition (LPCVD) of a stack of 300 nm amorphous silicon (a-Si) and 500 nm silicon dioxide (SiO$_2$). The a-Si passivation layer inhibits the conductive layer that intrinsically appears at the Si/SiO$_2$ interface, therefore reducing the substrate dielectric loss [11]. The thermal budget used in the following steps of the process is limited to values <500 °C, preventing the risk of recrystallization of the a-Si layer. A 360 nm VO$_2$ thin film is deposited by reactive magnetron

**Table 1**
Comparison of VO$_2$ tunable microwave filters.

| Reference | Givernaud et al., 2008 [6] | Bouyge et al., 2009 [7] | Bouyge et al., 2010 [8] | This work (thermal actuation, measurements) | This work (electrothermal actuation, simulations) |
|---|---|---|---|---|---|
| Function | Switchable bandstop | Tunable bandpass | Tunable bandstop | Tunable bandstop | Tunable bandstop |
| Area | 31.5 mm$^2$ | 63 mm$^2$ | 17.5 mm$^2$ | 4.4 mm$^2$ | 4.4 mm$^2$ |
| Substrate | Al$_2$O$_3$(C) | Al$_2$O$_3$ (C) | Al$_2$O$_3$ (C) | Si/SiO$_2$ | Si/SiO$_2$ |
| Actuation method | $T = 80\,^\circ$C | $V_{act} = 60$ V | $T > T_{MIT}$ | $T = 80\,^\circ$C | $V_{act} = 81.75$ V |
| Frequency range | 9 to 16 GHz | 1 to 18 GHz | 1 to 16 GHz | 1 to 40 GHz | 1 to 40 GHz |
| Center frequency (OFF) | 12.5 GHz | 9.4 GHz | 9.7 GHz | 22.5 GHz | 26.76 GHz |
| Center frequency (ON) | n.a | 8.8 GHz (−6.4%) | 9 GHz (−7.2%) | 19.8 GHz (−12%) | 21.9 GHz (−18.2%) |
| Max. insertion loss (OFF) | −10 dB | −4.1 dB | −0.9 dB | −1.8 dB | −2.8 dB |
| Max. insertion loss (ON) | −9.5 dB | −4.1 dB | −1 dB | −1.8 dB | −1.9 dB |
| Min. rejection level (OFF) | −47 dB | −17 dB | −31.6 dB | −17.2 dB | −12 dB |
| Min. rejection level (ON) | n.a | −14.5 dB | −33.2 dB | −18.8 dB | −11.9 dB |